Materials Science and Engineering A 508 (2009) 190–194

Contents lists available at ScienceDirect

Materials Science and Engineering A

journal homepage: www.elsevier.com/locate/msea

(AlN + Mg_2Si)/Mg composites *in situ* synthesis and scale effect of particulate on damping capacity

Congfa Zhang, Tongxiang Fan*, Wei Cao, Di Zhang*

State Key Lab of Metal Matrix Composites, Shanghai Jiaotong University, Shanghai, 200240, PR China

ARTICLE INFO

Article history:
Received 10 October 2008
Received in revised form 16 December 2008
Accepted 21 January 2009

Keywords:
Magnesium alloys
Particulate reinforced composites
Damping
Scale effect

ABSTRACT

(AlN + Mg_2Si)/Mg composites with uniform distribution of reinforcing particulates have been *in situ* synthesized and the scale effect of reinforcing particulates on damping capacity is investigated. The results show that at room temperature, composites reinforced with coarser particulates exhibit higher damping capacity compared with that reinforced with finer ones at low strain amplitude due to dominant contribution of plastic zone damping, while composites reinforced with finer particulates exhibit higher damping capacity at high strain amplitude and high frequency due to dominant contribution of dislocation damping. As temperature increases, the difference of damping capacity between composites reinforced with different size particulates reduces due to high damping capacity mainly arising from the grain boundary sliding and particulate-matrix interface.

1. Introduction

There has been strong interest in developing high damping materials to suppress mechanical vibrations for social and economic reasons. For these purposes, many research works have been focused on the development of Mg matrix composites (Mg-MMCs), as pure magnesium is known to exhibit high damping capacity and the incorporation of suitable ceramic particles can make up for many mechanical and physical properties limitations of pure Mg [1–4]. These researches put emphasis on the effects of shape [1], weight percentage [2], coating [3] and kinds [4] of particulates on damping capacity. However, little research emphasizes on the scale effect of particulate although it is clear that particulate scale effect is important [5].

Generally speaking, Mg-MMCs are synthesized by using powder metallurgy [6], stir casting [7], pressureless infiltration [8], *etc.* These *ex situ* techniques may suffer from the thermodynamic instability of interfaces and poor wettability between the reinforcement and the matrix. Therefore, the *in situ* techniques have received more attentions since *in situ* MMCs exhibit thermodynamically stable reinforcements and cleaner and stronger bonding matrix-reinforcement interfaces [9]. To date, successful *in situ* Mg-MMCs are still limited in Mg_2Si/Mg [10], TiC/Mg [11] and TiB_2/Mg [12] composites due to the lack of available *in situ* reactive system.

In this paper, a new *in situ* Mg-MMC hybrid reinforced with AlN and Mg_2Si particulates is developed. A synthesized route and a method to control the reinforcing particulate scale in the *in situ* (AlN + Mg_2Si)/Mg composites are presented. Furthermore, the scale effect of reinforcing particulate on damping capacity is investigated and the involved damping mechanism is discussed.

2. Experimental

Industry pure magnesium ingot (≥99.93%), industry pure aluminum ingot (≥99.7%), and 0.5 μm Si_3N_4 powders are used as starting materials to synthesize 4.4 vol.%AlN and 10.6 vol.%Mg_2Si reinforced Mg-MMCs. The mass% of the starting materials Mg, Al and Si_3N_4 are 85%, 8.4% and 6.6%, respectively. The synthesizing process is as following: first, the charge of about 1 kg pure Mg and Al ingot, and Si_3N_4 powders enwrapped by pure Al foil are melted in vacuum oven at 700 °C. Then, the melt is moved into electrical resistance furnace under the protection of SF_6/CO_2 gas atmosphere and is stirred at 575 °C, at which the fraction of solid is 40% [13], for 15 min to assist uniform dispersion of Si_3N_4. Subsequently the melt is held at 850 °C for 30 min to ensure complete reaction between Si_3N_4 and Al. Next, two different processing routes are adopted. One is that the melt is cooled to 700 °C and stirred for 15 min, subsequently the melt is directly poured into steel mold to get the resultant composite, defined as *S1*; the other is that the melt is cooled to 575 °C and stirred for 15 min, then the melt is re-heated to 700 °C and poured into steel mold to get another resultant composite, defined as *S2*.

The microstructure is examined by optical microscopy. The crystalline phases are determined by X-ray diffraction (XRD) with Cu Kα radiation at 40 kV and 200 mA. Damping capacity is tested by using Dynamic Mechanical Thermal Analysis (IDMA 2980type) in

* Corresponding authors. Tel.: +86 21 54747779; fax: +86 21 34202749.
E-mail addresses: txfan@sjtu.edu.cn (T. Fan), zhangdi@sjtu.edu.cn (D. Zhang).

0921-5093/$ – see front matter © 2009 Elsevier B.V. All rights reserved.
doi:10.1016/j.msea.2009.01.060

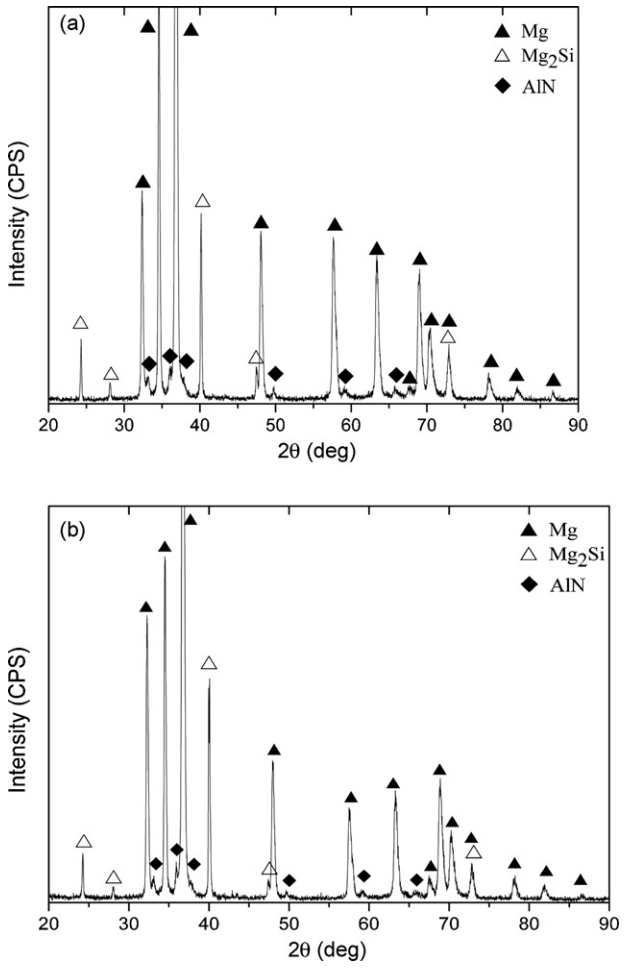

Fig. 1. X-ray diffraction patterns of (a) *S1*, composites reinforced with finer reinforcements and (b) *S2*, composites reinforced with coarser reinforcements.

single cantilever beam mode. The test-pieces for damping are as cast and machined with dimension of 40 mm × 5 mm × 1 mm on electric spark cutter. The test conditions are as following: the strain amplitude (ε_0) varies from 1×10^{-6} to 1×10^{-3}; the vibration frequency (f) is 0.1, 1 and 5 Hz, respectively; and the temperature (T) ranges from room temperature to 325 °C. The resulting sinusoidal force and deflection data are recorded and damping capacity is evaluated by the loss tangent ($\tan\varphi$). Larger $\tan\varphi$ indicates higher damping capacity.

3. Results and discussion

3.1. Microstructure and phase analysis

Fig. 1 shows XRD results of the composites sample *S1* and *S2*, respectively. The results reveal that the expected phases of AlN and Mg_2Si are formed and the starting Si_3N_4 is disappeared indicating Si_3N_4 is completely converted to AlN and Mg_2Si. Fig. 2 shows the microstructure of composites sample *S1* and *S2*, respectively. It can be seen that these composites yield a relatively uniform distribution of reinforcement particulates and Mg_2Si size in *S1* is about 30 μm while Mg_2Si size in *S2* is above 60 μm, AlN size is all about 0.5 μm in both *S1* and *S2*. When Si_3N_4 is completely converted to AlN, the Al and Si content are 3.6 wt.% and 4.3 wt.%, respectively. Based on 850 °C isothermal sections of Mg–Al–Si ternary phase diagram, it can be found that the melt (Mg–3.6 wt.%Al–4.3 wt.%Si) lies in the liquid phase area, so that Si released from Si_3N_4 is dissolved into the Mg alloy and Mg_2Si cannot be directly formed during the transition from Si_3N_4 to AlN. Therefore, reaction between Si_3N_4 and Mg–Al alloy takes place through $4[Al]_{\text{in Mg alloy}} + Si_3N_4(s) = 4AlN(s) + 3[Si]_{\text{i Mg alloy}}$. Mg_2Si particulates are formed during solidification. For composites *S1*, after pouring at 700 °C, Mg_2Si nucleation in the solidifying liquid alloy is difficult to initiate since effective nuclei are absent. As such, the melt needs to undercool. Until cooling to a specific temperature, Mg_2Si nucleation initiates and growth occurs. While for composite *S2*, great amount of Mg_2Si particles are formed during stirring at 575 °C after being held at 850 °C for 30 min. They cannot be completely dissolved in the period of re-heating to 700 °C to pour and are able to be as effective nuclei leading to Mg_2Si growth immediately after pouring. Therefore, relatively finer Mg_2Si particulates, as shown B in Fig. 2b, are formed in *S1* while coarser Mg_2Si particulates, as shown B in Fig. 2c and d, are formed in *S2*. AlN size is about sub-micron in both *S1* and *S2* since AlN size depends on the size of starting Si_3N_4 powders [14].

3.2. Damping capacity

Fig. 3 reveals a comparison of damping capacities between the resultant composites reinforced with different scale particulates at room temperature and different vibration frequency. At low strain amplitude, damping capacity of composite *S2* reinforced with coarser Mg_2Si particulates excels that of composite *S1* reinforced with finer ones; with increasing strain amplitude, damping capacities of both composite *S1* and *S2* are improved, meanwhile composite *S1* shows a quicker improving trend compared with composite *S2* with increasing frequency, and hence composite *S1* exhibits higher damping capacity than composite *S2* at $f = 5$ Hz. This phenomenon is attributed to the scale effect of reinforcing particulates. In MMCs, damping capacity mainly results from dislocation damping, depending on dislocation density, and plastic zone damping, depending on the volume fraction of plastic zone, at room temperature [1,15–17]. Reinforcing particulates of different scale generate different dislocation density at the matrix and different size of plastic zone around the particulate.

According to the Granato–Lücke (GL) dislocation model [18,19], the dislocation line is likened to an elastically vibrating string fixed at the pinning points in the crystal lattice. Under the applied cyclic loading, the dislocation line extends out from the fixed points produced by pinning impurity atoms, precipitates or antiplane dislocations. For a very small stress, the dislocation string bows out and continues to bow out until the breakaway stress is reached. At the breakaway stress, dislocation string breaks away the weak pinning, and thereafter the further motion of the dislocation line undergoes higher vibration amplitude. The motion of the dislocation depends on the local stress field adjacent to the dislocation. The inverse quality factor, Q^{-1}, is given by

$$Q^{-1} = Q_a^{-1} + Q_f^{-1} \tag{1}$$

where

$$Q_a^{-1} = C_1 \frac{\rho b^2}{\varepsilon_0} \exp\left(-\frac{C_2}{\varepsilon_0}\right) \tag{2}$$

and

$$Q_f^{-1} = C_3 \frac{\rho f^2}{b^2} \tag{3}$$

where C_1, C_2 and C_3 are physical constants, ρ and b are the dislocation density and Burgers vector, respectively; and ε_0 and f are the vibration strain amplitude and frequency, respectively. Q_f^{-1} denotes the frequency-dependent part of the inverse quality factor, and Q_a^{-1} the amplitude-dependent part. It is noted that at low strain amplitudes, dislocation damping mainly results from

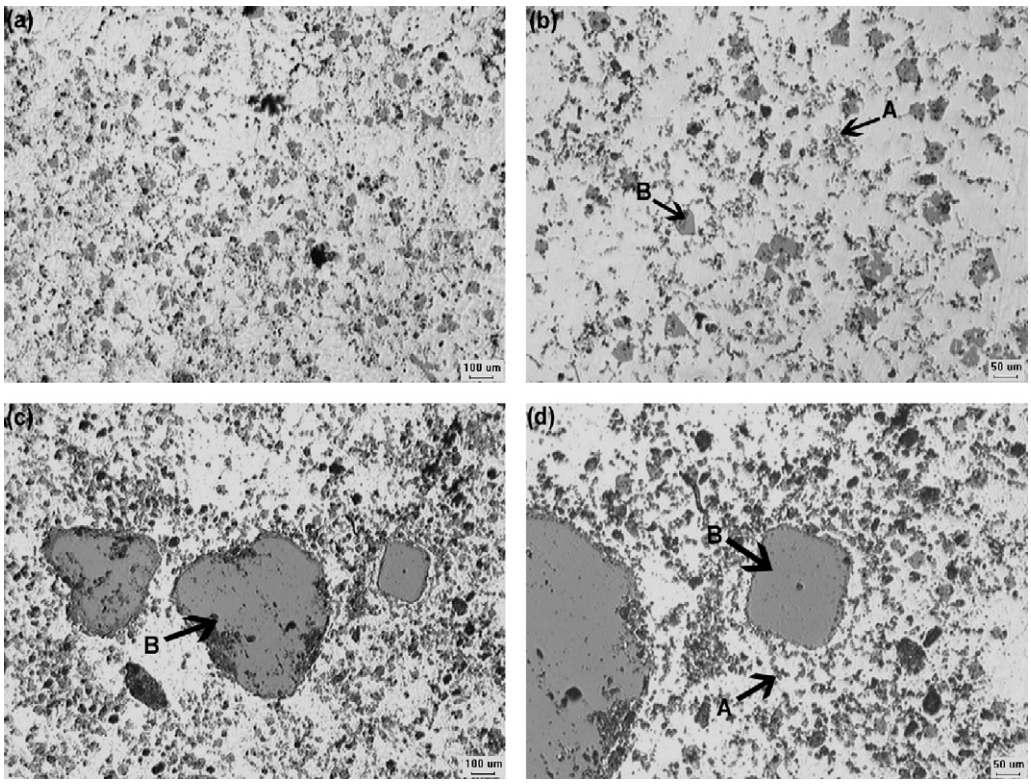

Fig. 2. Optical micrographs of composites (a), (b) composite *S1*, (c), (d) composite *S2* (A = AlN; B = Mg_2Si).

the frequency-dependent part, Q_f^{-1}, and beyond a critical strain amplitude, the strain amplitude-dependent part, Q_a^{-1}, becomes dominant. The occurrence of the critical strain amplitude is correspondent to the break-away of pinned dislocation string. From Eqs. (1) to (3), it is clear that dislocation damping is proportional to dislocation density and damping capacity improves with the increase of dislocation density.

Arsenault and Shi [20] further developed a simple model based on prismatic punching to calculate dislocation density as follows:

$$\rho = \frac{B\ \Delta\alpha\ \Delta T V_p}{bd(1-V_p)} \tag{4}$$

where B is a geometric constant (equals 12 for equiaxed particulates); $\Delta\alpha$ is the difference of CTE between Mg matrix alloy and reinforcements; ΔT is the difference between working temperature and final temperature which is around 510 K [13]; V_p is the volume fractions; b is the burgers vector which is around 0.3 nm [21], and d is the smallest dimension of the particle.

Another major source of damping is due to the presence of plastic zone. Carreno-Morelli et al. [22] proposed a simplistic model to determine the damping owing to the presence of plastic zone as follows:

$$\tan\ \phi \approx \frac{f_{zp} G \oint \sigma d\varepsilon}{\pi\sigma_o^2} \tag{5}$$

where f_{zp} is the plastic zone volume fraction, G is the shear modulus of the composite sample, σ_o is the alternating shear stress amplitude, σ and ε are the corresponding stress and strain, respectively, acting on the specimen. It is clear from Eq. (5) that plastic zone damping directly depends on the volume fraction of the plastic zone and improves with the increases of the volume fraction of the plastic zone.

Further, through solving the problem of a rigid mismatching sphere by using a solution developed for a growing hole with producing the same displacement at the sphere interface, Dunand and Mortensen [23], yielded that the size of the plastic zone C_s around the reinforcements can be estimated as

$$C_s = r_s\left(\frac{\Delta\alpha E\ \Delta T}{(1-\nu)\sigma_y}\right)^{1/3} \tag{6}$$

where σ_y is yield stress of metal matrix in tension, which is around 90 MPa [24]; E is the matrix elastic modulus, which is 45 GPa [24]; ν is the matrix Poisson's ratio, which is 0.35 [24]; and r_s is the particulate radius.

In the (AlN + Mg_2Si)/Mg MMCs, microstructure analysis shows that AlN size in *S1* and *S2* is similar and Mg_2Si size in *S1* and *S2* differs greatly. Therefore, the difference between damping capacity of *S1* and *S2* depends on scale effect of Mg_2Si particulates. Due to the large mismatch between the coefficients of thermal expansion of Mg ($25\times10^{-6}\,K^{-1}$) and AlN ($4.5\times10^{-6}\,K^{-1}$), Mg_2Si ($7.5\times10^{-6}\,K^{-1}$), high dislocation density in matrix and large plastic zone around the reinforcements are generated.

Based on Eq. (4), the dislocation density ρ in the matrix, generated by Mg_2Si particulates with volume fraction 10.6% and with the size about 30 μm in *S1*, is about $1.41\times10^{12}\,m^{-2}$, while the dislocation density ρ in the matrix, generated by Mg_2Si particulates with volume fraction 10.6% and with the size 60 μm in *S2*, is $7.05\times10^{11}\,m^{-2}$. However, according to the microstructure investigation, Mg_2Si particulates size in *S2* is above 60 μm, therefore, the dislocation density generated by Mg_2Si particulates in *S2* is below $7.05\times10^{11}\,m^{-2}$. Furthermore, based on Eq. (6), the radius of plastic zone around the Mg_2Si particulates with the size 30 μm in *S1* is 28.5 μm, while the radius of plastic zone around the Mg_2Si particulates with the size 60 μm in *S2* is 57 μm. Thus, it is clear that composite *S1* reinforced with finer Mg_2Si particulates has higher dislocation density and smaller plastic zone compared with composite *S2* reinforced with coarser ones. Further, this difference will decide that which one of *S1* and *S2* exhibits higher damping capacity

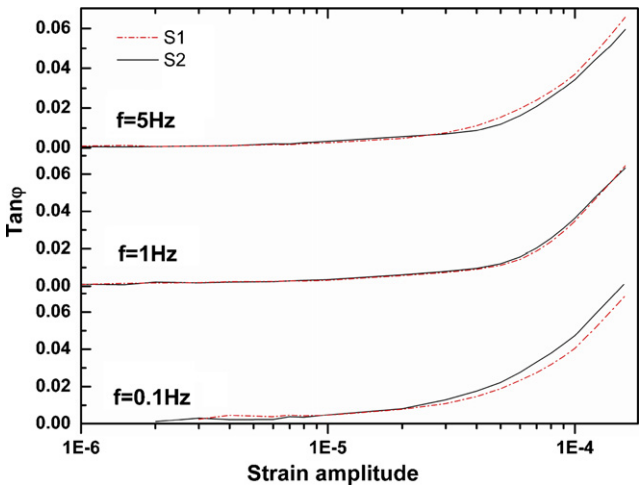

Fig. 3. Comparison of damping capacities of composites *S1* reinforced with finer particulates and *S2* reinforced with coarser particulates at room temperature and different frequency.

according as which damping mechanism is dominant contribution for the overall damping capacity.

According to GL dislocation model, under low strain amplitude type cyclic load dislocation bows out, but does not break away the pinning, dislocation damping mainly results from the frequency-dependent part and is small, plastic zone damping may be dominant contribution for the overall damping capacity. Therefore, composite *S2* reinforced with coarser particulates, which has larger size of plastic zone, exhibits higher damping capacity compared with composite *S1*. According to reference [16,22], plastic zone damping is inversely proportional to the vibration frequency. In addition, according to GL dislocation model as strain amplitude increases to the critical strain amplitude, the dislocations may break away in a snowslide-like mode from the weak pinning and the dislocation damping increases quickly. Thus, at high strain amplitude and high vibration frequency the dislocation damping mechanism becomes dominant. As a result, composite *S1* reinforced with finer particulates, which has higher dislocation density, exhibits higher damping capacity.

Fig. 4 shows a comparison of damping capacities of the resultant composites reinforced with different scale particulates at $\varepsilon_0 = 2 \times 10^{-5}$ and different vibration frequency. It is noted that at low temperature the damping capacity of composite *S2* is higher than

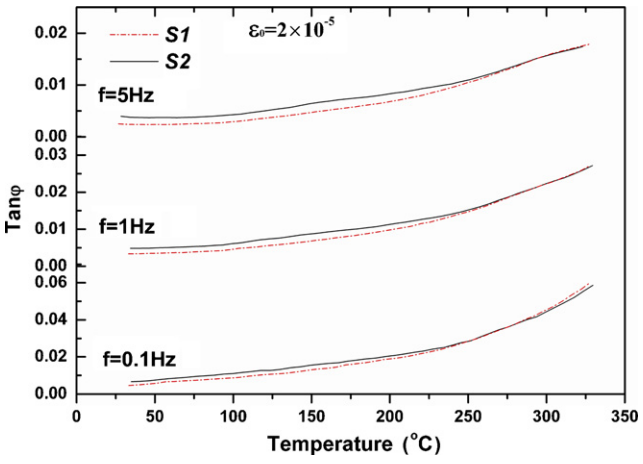

Fig. 4. Comparison of damping capacities of composites *S1* reinforced with finer particulates and *S2* reinforced with coarser particulates *vs*. temperature at different frequency.

that of *S1*; with increasing temperature, the difference of damping capacities between composite *S1* and *S2* reduces. This indicates that the scale effect of reinforcing particulates on damping capacity reduces with increasing temperature.

The testing strain amplitude, ε_0, is 2×10^{-5} and is less than critical strain amplitude. Combined with the former discussion, it can be noted that plastic zone damping mechanism is dominant at this strain amplitude and hence composite *S2*, which has larger plastic zone, exhibits higher damping capacity than *S1* at low temperature. As temperature increases, damping capacity of composites improves mainly arising from grain boundary sliding and particulate-matrix interface [3]. In addition, according to Eqs. (4) and (6), the dislocation density and the size of plastic zone decrease and the difference of them between composite *S1* and *S2* reduces with increasing temperature, thus, the contribution of dislocation damping and plastic zone damping falls. Therefore, the scale effect of reinforcing particulates on damping capacity reduces with increasing temperature. Some researchers [4] have pointed out that the high temperature damping peak may be present. As the temperature increases, the bonding strength of the interface becomes lower. The displacement of the interface slip increases, and the energy consumed by interface slip may still increase. When the temperature increases too much, although the displacement of interface slip still increases, the strength of the interface bonding is so low that the energy consumed may no longer increase. Therefore, the optimum bonding strength of the interface may exist at a proper temperature, which leads to a maximum energy loss, and thus a damping peak of interface slip may be formed. However, in composite *S1* and *S2*, there is not obviously high temperature damping peak. This is due to strength interface bonding between the *in situ* formed reinforcements and matrix until high temperature.

4. Conclusions

An *in situ* synthesizing route of $(AlN + Mg_2Si)/Mg$ composites starting from Si_3N_4 powders and Mg–Al alloys has been presented. Reinforcing particulates of different scale have been formed through controlling their nucleation and growth.

At room temperature, at low strain amplitude composites reinforced with coarser particulates, which have larger plastic zone, exhibit higher damping capacity since plastic zone damping dominates. With increasing strain amplitude and frequency, the dislocation damping becomes dominant and hence composites reinforced with finer ones, which have higher dislocation density, exhibit higher damping capacity.

With increasing temperature, the scale effect of reinforcing particulates on damping capacity becomes to be no evident due the high damping capacity of composites mainly arising from grain boundary sliding and particulate-matrix interface. High temperature damping peak is absent due to strength interface bonding between the *in situ* formed reinforcements and matrix.

The research is attractive since it deduces that in a specific MMCs, high damping capacity can be obtained in a wide vibration frequency range from low frequency to high frequency by the combination of reinforcing particulates of hierarchical size.

Acknowledgements

The authors are grateful for the financial supports from Toyota Cooperation Foundation, National Nature Science Foundation of P.R. China (No.50671064), Key Basic Research Program of Shanghai (No.88JC1411400) and Shanghai Rising-Star Program (No.05QMX1434).

The authors also wish to thank Dr. Akira Kato, Dr. Tomoyasu Kitano, Dr. Katsutoshi Noda, Dr. Akira Manabe in Toyota for their valuable discussion in the course of this research.

References

[1] L.H. Liao, H.W. Wang, X.F. Li, N.H. Ma, Mater. Lett. 61 (2007) 2518.
[2] N. Srikanth, C.H. Gaofeng, M. Gupta, J. Alloys Compd. 352 (2003) 106.
[3] J.H. Gu, X.N. Zhang, Y.F. Qiu, M.Y. Gu, Compos. Sci. Technol. 65 (2005) 1736.
[4] J.H. Gu, X.N. Zhang, M.Y. Gu, J. Alloys Compd. 385 (2004) 104.
[5] G. Garcés, M. Rodríguez, P. Pérez, P. Adeva, Mater. Sci. Eng. A 419 (2006) 357.
[6] Y. Morioka, J. Jpn. Soc. Powder Powder Metall. 40 (1993) 755.
[7] T. Imai, S.W. Lim, D. Jiang, Y. Nishida, Scripta Mater. 36 (1997) 611.
[8] C.A. Leo'n, Y. Arroyo, E. Bedolla, E.A. Aguilar, R.A.L. Drew, Mater. Sci. Forum 509 (2006) 105.
[9] S.C. Tjong, Z.Y. Ma, Mater. Sci. Eng. R 29 (2000) 49.
[10] M. Mabuchi, K. Kubota, K. Higashi, J. Mater. Sci. 31 (1996) 1529.
[11] K. Yamada, T. Takahashi, M. Motoyama, J. Jpn. Inst. Met. 60 (1996) 100.
[12] M.A. Matin, L. Lu, M. Gupta, Scripta Mater. 45 (2001) 479.
[13] A. Tissier, D. Apelian, G. Regazzoni, J. Mater. Sci. 25 (1990) 1184.
[14] M.K. Aghajania, J.P. Biel, R.G. Smith, J. Am. Ceram. Soc. 77 (1994) 1917.
[15] N. Srikanth, M. Gupta, Mater. Res. Bull. 37 (2002) 1149.
[16] N. Srikanth, D. Saravanaranganathan, M. Gupta, Mater. Sci. Technol. 20 (2004) 1389.
[17] N. Srikanth, X.L. Zhong, M. Gupta, Mater. Lett. 59 (2005) 3851.
[18] A. Granato, K. Lüecke, J. Appl. Phys. 27 (1956) 583.
[19] A. Granato, K. Lüecke, J. Appl. Phys. 27 (1956) 789.
[20] R.J. Arsenault, N. Shi, Mater. Sci. Eng. A 81 (1986) 175.
[21] H.J. Frost, M.F. Ashby, Deformation-Mechanism Maps: The Plasticity and Creep of Metals and Ceramics, Pergamon Press, Oxford, 1982.
[22] E. Carreno-Morelli, S.E. Urreta, R. Schaller, Acta Mater. 48 (2000) 4725.
[23] D. Dunand, A. Mortensen, Mater. Sci. Eng. A 135 (1991) 179.
[24] J. Zhang, Z.H. Zhang, Mg Alloys and Application, Chemical Industry Press, Beijing, 2004.